AASLD
AMERICAN ASSOCIATION FOR
THE STUDY OF LIVER DISEASES

ORIGINAL ARTICLE

Persistent biliary hypoxia and lack of regeneration are key mechanisms in the pathogenesis of posttransplant nonanastomotic strictures

Iris E. M. de Jong[1,2] | Diletta Overi[3] 🟢 | Guido Carpino[4] 🟢 |
Annette S. H. Gouw[5] | Marius C. van den Heuvel[5] | Léon C. van Kempen[5] |
Carmine Mancone[6] | Paolo Onori[3] | Vincenzo Cardinale[7] | Luca Casadei[8] |
Domenico Alvaro[9] | Robert J. Porte[2] | Eugenio Gaudio[3]

[1]Surgical Research Laboratory, Department of Surgery, University of Groningen, University Medical Center Groningen, Groningen, The Netherlands

[2]Section of Hepatobiliary Surgery and Liver Transplantation, Department of Surgery, University of Groningen, University Medical Center Groningen, Groningen, The Netherlands

[3]Department of Anatomical, Histological, Forensic Medicine and Orthopedic Sciences, Sapienza University of Rome, Rome, Italy

[4]Division of Health Sciences, Department of Movement, Human and Health Sciences, University of Rome "Foro Italico", Rome, Italy

[5]Department of Pathology, University of Groningen, University Medical Center Groningen, Groningen, The Netherlands

[6]Department of Molecular Medicine, Sapienza University of Rome, Rome, Italy

[7]Department of Medico-Surgical Sciences and Biotechnologies, Polo Pontino, Sapienza University of Rome, Rome, Italy

[8]Department of Chemistry, Sapienza University of Rome, Rome, Italy

[9]Department of Translational and Precision Medicine, Sapienza University of Rome, Rome, Italy

Correspondence
Robert J. Porte, Section of Hepatobiliary
Surgery and Liver Transplantation,
Department of Surgery, University Medical
Center Groningen, P.O. Box 30.001, 9700
RB Groningen, The Netherlands.
Email: r.j.porte@umcg.nl

Abstract

Background and Aims: Nonanastomotic biliary strictures (NAS) are a major cause of morbidity after orthotopic liver transplantation (OLT). Although ischemic injury of peribiliary glands (PBGs) and peribiliary vascular plexus during OLT has been associated with the later development of NAS, the exact underlying mechanisms remain unclear. We hypothesized that bile ducts of patients with NAS suffer from ongoing biliary hypoxia and lack of regeneration from PBG stem/progenitor cells.

Abbreviations: BTSC, biliary tree stem cell; CholM, cholangiocyte medium; CK7, cytokeratin 7; DBD, donation after brain death; DCD, donation after circulatory death; DR, ductular reaction; EC, endothelial cell; ERCP, endoscopic retrograde cholangiopancreatography; FFPE, formalin-fixed, paraffin-embedded; HAT, hepatic artery thrombosis; H&E, hematoxylin and eosin; Hep-Par1, hepatocyte paraffin 1; HIF-1α, hypoxia-inducible factor 1 alpha; IF, immunofluorescence; IHC, immunohistochemistry; KM, Kubota's medium; MVD, microvascular density; NAS, nonanastomotic strictures; NCAM, neural cell adhesion molecule; NMR, nuclear magnetic resonance; OLT, orthotopic liver transplantation; PAS, periodic acid Schiff; PBG, peribiliary gland; pCK, pan-cytokeratin; PCNA, proliferating cell nuclear antigen; PHD2, prolyl hydroxylase domain-containing protein 2; PVP, peribiliary vascular plexus; SCTR, secretin receptor; SHH, sonic hedghog; αSMA, α-smooth muscle actin; Sox9, SRY-box transcription factor 9; SR/FG, Sirius Red/Fast Green; SQ, semiquantitative; Thy-1, thymus cell surface antigen 1; TUNEL, terminal deoxynucleotidyl transferase dUTP nick end labeling; UMCG, University Medical Center Groningen; VEGF-R2, VEGF receptor 2; VWF, von Willebrand factor.

Iris E.M. de Jong and Diletta Overi share first authorship.

Robert J. Porte and Eugenio Gaudio share senior authorship.

Approach and Results: Forty-two patients, requiring retransplantation for either NAS (*n* = 18), hepatic artery thrombosis (HAT; *n* = 13), or nonbiliary graft failure (controls; *n* = 11), were included in this study. Histomorphological analysis of perihilar bile ducts was performed to assess differences in markers of cell proliferation and differentiation in PBGs, microvascular density (MVD), and hypoxia. In addition, isolated human biliary tree stem cells (hBTSCs) were used to examine exo-metabolomics during in vitro differentiation toward mature cholangiocytes.

Bile ducts of patients with NAS or HAT had significantly reduced indices of PBG mass, cellular proliferation and differentiation (mucus production, secretin receptor expression, and primary cilia), reduced MVD, and increased PBG apoptosis and hypoxia marker expression, compared to controls. Metabolomics of hBTSCs during in vitro differentiation toward cholangiocytes revealed a switch from a glycolytic to oxidative metabolism, indicating the need for oxygen.

Conclusions: NAS are characterized by a microscopic phenotype of chronic biliary hypoxia attributed to loss of microvasculature, resulting in reduced proliferation and differentiation of PBG stem/progenitor cells into mature cholangiocytes. These findings suggest that persistent biliary hypoxia is a key mechanism underlying the development of NAS after OLT.

INTRODUCTION

Biliary complications remain a major cause of morbidity and graft loss after orthotopic liver transplantation (OLT).[1] These complications are collectively identified as posttransplant cholangiopathy, and they may vary from anastomotic strictures and bile leakage to nonanastomotic biliary strictures (NAS), or even bile duct necrosis and intrahepatic biloma formation.[2] NAS are generally defined as irregularities and strictures of the large intra- and extrahepatic donor bile ducts, leading to recurrent cholestasis and/or cholangitis, in the presence of a patent hepatic artery.[2,3] OLT recipients who develop NAS may have had an apparently uncomplicated transplant procedure, but typically present themselves with recurrent cholestasis and/or cholangitis at a median of 3-4 months postoperatively.[4] The diagnosis of NAS is generally made on imaging of the biliary tree (i.e., endoscopic cholangiography or MR cholangiography). Although biliary injury attributable to ischemia and/or bile salt toxicity during the transplant process has been associated with the occurrence of NAS,[5,6] the exact pathogenesis underlying its development remains unclear. The nourishment of the biliary tree depends on the peribiliary vascular plexus (PVP) that derives from the hepatic artery.[7,8] Hepatic artery thrombosis (HAT) after OLT frequently leads to the formation of biliary strictures, but in the case of NAS the hepatic artery is shown to be patent.[2]

The regeneration of large intra- and extrahepatic bile ducts is supported by the peribiliary glands (PBGs).[9] PBGs are seromucous glands that harbor a niche of stem/progenitor cells, the so-called biliary tree stem/progenitor cells (BTSCs).[10,11] These cells are characterized by high self-replication capabilities and the capacity to regenerate cholangiocytes and restore damaged biliary surface epithelium.[9,12,13] However, in pathological conditions, PBGs may be severely compromised and unable to exert their regenerative function.[9,14] It has been suggested that insufficient regeneration because of loss of PBGs and/or microvascular damage may explain the development of NAS after OLT.[6] Although bile duct injury at the time of OLT has been linked with the development of NAS, there are no studies that have examined the histopathological phenotype of end-stage NAS. We hypothesized that bile ducts with NAS suffer from ongoing (microscopic) biliary hypoxia and lack of regeneration from PBG stem/progenitor cells, despite a patent hepatic artery. To test this hypothesis, we performed a histomorphological analysis of organs requiring retransplantation for NAS, HAT, or nonbiliary causes of graft failure (controls). In this analysis, we focused on: (1) pathological changes with an emphasis on the PVP and PBGs; (2) epithelial regeneration; (3) fibrotic changes; and (4) activation of ischemia-related pathways.

PATIENTS AND METHODS

Patients

A total of 42 adult OLT recipients, who required retransplantation of the liver at the University Medical Center Groningen (UMCG) between 1990 and 2016, were included in this study. Patients with primary sclerosing cholangitis were excluded. Eighteen patients required retransplantation for NAS within 1 year from the first OLT (NAS group), 13 were retransplanted for HAT (HAT group), and 11 patients required a retransplant for nonbiliary causes, such as recurrence of viral or autoimmune hepatitis (controls).

In patients with NAS, imaging of the biliary tree was indicated based on clinical symptoms (i.e., fever, chills, or jaundice), in combination with laboratory values indicating biliary pathology. NAS was diagnosed by endoscopic retrograde cholangiopancreatography (ERCP), magnetic resonance cholangiopancreatography (MRCP), or percutaneous transhepatic cholangiography (PTC) and defined as strictures, dilatations, or irregularities of the intra- or extrahepatic donor bile ducts in the absence of HAT. HAT was excluded by Doppler ultrasound. Isolated strictures at the bile duct anastomosis were excluded. Radiological locations of NAS in the biliary tree were classified as described by Buis et al.[4] Early HAT was defined as absence of hepatic artery flow on Doppler ultrasound or computer tomography within 40 days after OLT and always confirmed during the retransplant procedure.

Light microscopy, immunohistochemistry, and immunofluorescence

Formalin-fixed, paraffin-embedded (FFPE) sections of explanted donor bile ducts and livers were obtained from the Pathology Department of the UMCG. All samples were taken from the hilar region of explanted liver and included cross-sectional representations of extrahepatic ducts as well as large intrahepatic bile ducts, with or without surrounding tissues. Three- to 4-μm sections were prepared and stained with hematoxylin and eosin (H&E), periodic acid Schiff (PAS), Sirius Red/Fast Green (SR/FG), and Masson's trichrome stain, according to standard protocols.[15] Degree of necrosis, inflammation, and fibrosis was assessed in routine stains.

For immunohistochemistry (IHC), endogenous peroxidase activity was blocked by a 30-minute incubation in methanolic hydrogen peroxide (2.5%). Antigens were retrieved by applying Proteinase K (code S3020; Dako, Glostrup, Denmark) for 10 minutes at room temperature. Sections were then incubated overnight at 4°C with primary antibodies (Table S1). Sections were incubated with secondary biotinylated antibody and then with Streptavidin-HRP (LSAB+ System-HRP, code

K0690; Dako). Diaminobenzidine (code K3468; Dako) was used as substrate; sections were counterstained with hematoxylin.

To assess apoptosis, terminal deoxynucleotidyl transferase dUTP nick end labeling (TUNEL) assay (ApopTag Peroxidase In Situ Apoptosis Detection Kit; Merck Millipore, Burlington, MA) was performed according to the manufacturer's protocol.

For immunofluorescence (IF), nonspecific protein binding was blocked by 5% normal goat serum. Specimens were incubated with primary antibodies, incubated for 1 hour with labeled isotype-specific secondary antibodies (Alexa Fluor; Invitrogen, Life Technologies Ltd, Paisley, UK), and, finally, counterstained with DAPI for visualization of cell nuclei. Adequate negative controls were included for all immunostainings.

Slides were examined in a coded fashion using a Leica Microsystems DM4500B Light and Fluorescence Microscope (Leica Microsystems, Wetzlar, Germany) and were scanned by a digital scanner (Aperio Scanscope CS/FL System, Aperio Digital Pathology; Leica Biosystems, Milan, Italy) and processed by ImageScope.

Ductular reaction (DR) in liver sections and the area occupied by PBGs (PBG mass) in bile ducts were evaluated in cytokeratin 7 (CK7)-stained sections and are expressed as the percentage of the total analysis area.[13] The number of destroyed PBG acini was counted as a percentage of the total number of acini; this percentage was converted in a semiquantitative (SQ) score (0 = <1%; 1 = 1%-10%; 2 = 10%-30%; 3 = 30%-50%; and 4 = >50%). Microvascular density (MVD) was calculated as the area occupied by von Willebrand factor (vWF)$^+$ and CD31$^+$ vessels. Moreover, vessels were counted and expressed as number of vessels per microscopic field at 20×. Wall thickness was measured on SR-stained slides; the amount of SR$^+$ fibers within the bile duct wall was quantified by a computer algorithm and is expressed as area percentage. The number of CD68$^+$ macrophages and α-smooth muscle actin (αSMA)$^+$ cells was counted and is expressed as number of cells per microscopic field at 40×. The number of positive cells in PBGs was automatically calculated by a computer algorithm; nuclear positivity is expressed as percentage of positive cells; for cytoplasmic stains, the previously mentioned SQ score was applied. The number of cells displaying a primary cilium was evaluated on α-acetylated tubulin–stained slides and is expressed as SQ score.

Quantitative PCR analysis

Representative tissue samples of NAS (n = 3), HAS (n = 3), and control patients (n = 2) were selected for gene expression analysis. Regions of interest indicated by a pathologist (M.C.v.d.H.) were macrodissected from four 10-μm FFPE sections. Subsequently, total

RNA was isolated using Qiagen's RNeasy FFPE kit (Qiagen, Hilden, Germany), according to the supplier's instruction, and quantified using a Qubit Fluorometer (Invitrogen, ThermoFisher Scientific, Waltham, MA, USA). Complementary DNA (cDNA) was generated with Superscript II (Invitrogen), random hexamer primers (Invitrogen), and 500-μg total RNA input according to the supplier's protocol. Per PCR reaction, 2.5 μL of 4× diluted cDNA was used in a TaqMan Gene expression assay (Applied Biosystems, ThermoFisher Scientific) with fluorescently labeled primers (ThermoFisher Scientific; Table S2) in a total volume of 10 μL. The Pfaffl method was used to calculate expression of the gene of interest relative to the expression of peptidyl-prolyl isomerase A while accounting for differences in primer efficiencies.[16]

Exo-metabolomics of Isolated Human BTSCs

Human BTSCs were isolated from the extrahepatic biliary tree and cultured in a self-replication medium (i.e., Kubota's Medium [KM]), as described.[17,18] For differentiation studies, cells were transferred in a medium for cholangiocyte differentiation (CholM) prepared by supplementing KM with calcium (final concentration, 0.6 mM), copper (10^{-12}M), 20 ng/mL of basic fibroblast growth factor, 20 ng/mL of VEGF165, and 10 ng/mL of hepatocyte growth factor.[18] One milliliter of culture medium was freeze-dried for 24 hours. The resulting powder was dissolved in 600 mL of phosphate D2O buffer solution (pH 7.4), 3-(trimethylsilyl)propionic-2,2,3,3-d4 acid sodium 1 mM, and NaN_3 10 mM. For the analysis of medium samples, the ^{1}H nuclear magnetic resonance (NMR) spectra were acquired on a Varian VNMRS 500 spectrometer at the frequency of 500 MHz using a two-dimensional J-resolved pulse sequence.[19] After processing the NMR data, principal component analysis was performed using SIMCA-P+ software (v.12; Umetrics, Umeå, Sweden).

Statistical analysis

Continuous data are presented as mean ± SD or as median and interquartile range. A one-way ANOVA test was used to calculate differences between the three groups. When a difference was identified by the one-way ANOVA test, a Bonferroni *post hoc* test was applied to calculate the p value. The Pearson correlation coefficient or the Spearman nonparametric correlation was used to determine the relationship between two variables. A p value <0.05 was considered statistically significant. Analyses were performed using IBM SPSS software (IBM, Armonk, NY).

RESULTS

Donor and recipient characteristics

Clinical, biochemical, and surgical characteristics of donors and patients requiring retransplantation for nonbiliary indications (controls), NAS or HAT are presented in Table 1. Indications for retransplantation in the control group are summarized in Table S3. There were no significant differences in donor characteristics among the three groups, apart from a higher proportion of livers donated after circulatory death in the NAS group. NAS was diagnosed at a median of 82 (40-124) days after the first OLT. The time interval between the diagnosis of NAS and retransplantation was 280 (109-2,042) days. As expected, the time interval between the first and second OLT varied between the three groups. In the control group, livers were retransplanted at a median of 1,512 (854-3,040) days after the initial OLT, whereas this time interval was 386 (143-2,293) days in the NAS group and 7 (5-31) days in the HAT group. Serum values of liver function tests also differed among the three groups, as could be expected based on the underlying pathology.

Clinical and radiological characteristics of patients undergoing retransplantation for NAS are summarized in Table 2 and Figure 1A. All patients with NAS had strictures in zones A or B of the biliary tree, defined as the extrahepatic common bile duct and the extrahepatic part of the hepatic ducts, and the area between the intrahepatic hepatic ducts and second-order branches (i.e., segmental intrahepatic bile ducts), respectively.[4] Smaller biliary branches (i.e., area and septal intrahepatic bile ducts), more proximal from these levels (zones C and D), were generally not affected. Before retransplantation, most of the patients with NAS had undergone multiple interventions such as ERCP and PTC drainage. Moreover, most patients who suffered from NAS presented with one or more episodes of cholangitis.

Liver histopathology in controls, NAS and HAT

Histologically, liver parenchyma in all samples was characterized by a variable degree of necrosis, inflammation, and fibrosis (Table S4; Figure S1). Liver parenchymal necrosis ($F = 0.372$; $p = 0.695$) and inflammation ($F = 0.803$; $p = 0.464$) did not differ between examined groups (i.e., control, HAT, and NAS). Livers transplanted for nonbiliary graft failure presented with bridging fibrosis or established cirrhosis in the parenchyma. However, the histology of large intrahepatic bile ducts and hepatic ducts of these patients showed similarities with healthy ducts obtained from patients without liver or biliary diseases (see data in Figure S2).

TABLE 1 Clinical and surgical characteristics of donors and recipients

Variable	Control (n = 11)	NAS (n = 18)	HAT (n = 13)	p Values
Donor characteristics				
Age (years)	50 (45-53)	45 (39-56)	53 (49-59)	0.69
Sex				
Male	2 (20%)	10 (56%)	5 (42%)	0.2
Female	8 (80%)	8 (44%)	7 (58%)	
GGT (U/L)	14 (9-31)	20 (17-59)	27 (14-83)	0.25
Type of donor				
DCD	0	7 (39%)	1 (8%)	**0.03**[c]
DBD	9 (82%)	11 (61%)	11 (85%)	
Cold ischemia time (hour:minute)	10:02 (7:39-13:52)	8:34 (7:21-10:37)	8:19 (7:06-10:06)	0.22
Warm ischemia time (hour:minute)	0:54 (0:46-0:57)	0:51 (0:39-1:02)	0:47 (0:35-0:55)	0.31
Recipient characteristics				
Age (years)[a]	41 (22-50)	47 (35-56)	52 (40-56)	0.13
Sex				
Male	5 (45%)	7 (39%)	5 (38%)	0.93
Female	6 (55%)	11 (61%)	8 (62%)	
MELD score	20 (15-23)	22 (15-25)	19 (12-23)	0.29
Days between first and second transplant	1,512 (854-3,040)	386 (143-2,293)	7 (5-31)	**0.01**[d]
Bile duct anastomosis at first OLT				
Duct to duct	11 (100%)	16 (89%)	9 (70%)	0.22
Hepaticojejunostomy	0	2 (11%)	3 (23%)	
Surgical technique				
Classical	4 (36%)	3 (17%)	1 (8%)	0.35
Piggyback	6 (55%)	15 (83%)	12 (92%)	
Laboratory serum values[b]				
AST (U/L)	55 (30-148)	105 (70-157)	366 (90-2,036)	0.07
ALT (U/L)	54 (19-100)	69 (54-117)	614 (88-2,262)	**0.00**[d,e]
GGT (U/L)	91 (58-431)	344 (202-734)	92 (52-380)	0.3
ALP (U/L)	133 (78-265)	484 (205-756)	143 (111-244)	0.24
Bilirubin (µmol/L)	53 (15-607)	169 (55-274)	49 (20-111)	0.37
Albumin (g/L)	34 (29-35)	34 (29-38)	18 (12-25)	**0.00**[d,e]

Note: Data are expressed as median and interquartile range; *p* values <0.05 are in bold. In some groups, numbers do not add up because of missing data.

[a]At time of first transplant.

[b]Before retransplantation.

[c]*Post hoc* test showed a *p* < 0.05 between control and NAS groups.

[d]*Post hoc* test showed a *p* < 0.05 between control and HAT groups.

[e]*Post hoc* test showed a *p* < 0.05 between NAS and HAT groups.

Abbreviations: MELD, Model for End-Stage Liver Disease; ALP, alkaline phosphatase; AST, aspartate aminotransferase; ALT, alanine aminotransferase; GGT, gamma glutamyl transferase.

HAT livers showed less fibrosis (1.0 ± 0.9) compared to the NAS (2.1 ± 0.4; *p* = 0.035) and control group (3.8 ± 0.4; *p* < 0.001), with the latter presenting the highest value (*p* < 0.001 vs. NAS). Finally, the extent of DR was lower in HAT (0.7 ± 0.5%) and NAS (1.2 ± 0.6%) livers compared to controls (3.5% ± 1.9%; *p* = 0.002 and *p* = 0.008, respectively), whereas DR did not significantly differ between NAS and HAT livers. DR significantly correlated with liver fibrosis (*r* = 0.660; *p* = 0.003).

Bile duct histopathology in controls, NAS, and HAT

H&E stains of bile ducts in the three groups revealed morphological differences. Bile ducts of control livers showed an intact surface epithelium and compact PBG clusters. Histological specimens derived from patients in the NAS group were heterogeneous, but were generally characterized by a loss of surface

TABLE 2 Clinical and radiological characteristics of patients in the NAS group

Variable	No. (%)
Radiological localization of NAS[a]	
Zone A	15 (83)
Zone B	3 (17)
Zone C	0
Zone D	0
History of bile leakage	
Yes	7 (39)
No	11 (61)
Appearance of casts and/or sludge on ERCP/ MRCP	
Cast(s), sludge, or both	6 (33)
Not present or not described	12 (67)
Interventions preceding retransplant	
None	1 (6)
ERCP without balloon dilatation and stenting	2 (11)
ERCP with balloon dilatation and/or stenting	4 (22)
ERCP + PTCD	5 (28)
Surgery	1 (6)
ERCP + surgery	4 (22)
PTCD + ERCP + surgery	1 (6)
Episodes of cholangitis	
None	6 (33)
1-2	4 (22)
Recurrent cholangitis (>2)	8 (44)

Note: Data are expressed as numbers with percentage.

[a]Based on classification described by Buis et al.[4]

Abbreviation: PTCD, percutaneous transhepatic cholangiodrainage.

biliary epithelium and destruction of PBGs. The pre-transplant number of episodes of cholangitis (Table 2) did not affect the histological score in the NAS group. The HAT group was characterized by loss of surface epithelial cells, detachment of PBG cells from their basement membrane, and presence of microthrombi in the PVP, as well as intramural bleeding in some specimens (Figure 1B). The NAS group was characterized by a higher degree of inflammation, compared to controls ($p = 0.023$). Moreover, the NAS and HAT groups (8.9 ± 4.6 and 9.7 ± 2.9, respectively; Table S5) showed a higher number of macrophages infiltrated in the duct wall compared to the control group (0.30 ± 0.05, $p < 0.05$; Figure 1B,C).

PBG damage in NAS and HAT

PBGs in NAS and HAT groups showed signs of severe injury (i.e., PBG dilatation and disruption). PBG mass was significantly lower in NAS (1.7% ± 0.8%) and HAT (1.9% ± 1.4%) groups, compared to controls (4.3 ± 1.9;

$p = 0.039$ and $p = 0.029$, respectively; Figure 1B,C). In accordance with this, the count of disrupted glands in the NAS (score, 2.4 ± 1.2) and HAT (score, 2.5 ± 0.9) groups were significantly higher, compared to controls (score, 0.5 ± 0.6; $p = 0.021$ and $p = 0.013$, respectively; Figure 1B,C). No significant differences in PBG mass or injury were found between NAS and HAT groups. In NAS samples, no significant differences were found among patients who received a DCD (donation after circulatory death) versus DBD (donation after brain death) organ during the first OLT.

Histological specimens, taken from the perihilar region, included hepatic ducts and segmental bile ducts, as well as liver parenchyma, where area, septal, and interlobular bile ducts were present. In the NAS group, when included in the section, area intrahepatic bile ducts did not display significant histological injury (Figure S3). This enabled us to compare the histology of affected and nonaffected bile ducts in patients with NAS. NAS-affected ducts were characterized by a lower PBG mass (1.6% ± 0.8%) and a higher percentage of destroyed PBGs (score, 2.9 ± 1.3), compared to nonaffected ducts (6.9% ± 4.0%; score, 0.5 ± 0.5; $p <$ 0.001; Figure S3). PBG mass and percentage destroyed PBGs of nonaffected ducts in patients with NAS did not differ from bile ducts in the control group. Therefore, in the following analyses, data were obtained from NAS-affected ducts.

PBG proliferation, apoptosis, and senescence in NAS and HAT

Proliferation index of PBG cells was assessed by double immunostaining of proliferating cell nuclear antigen (PCNA) and pan-cytokeratin (pCK; Figure 2A,C). In parallel with differences in PBG mass, the proliferation index was significantly lower in ducts with NAS (19.9% ± 7.8%) or HAT (23.5% ± 7.0%), compared to controls (40.5% ± 17.9%; $p = 0.012$ and $p = 0.042$, respectively). Differences found in PBG mass and PCNA expression on a protein level were confirmed on an RNA level by quantitative PCR (Figure S4A,B). No significant differences were found between the NAS and HAT groups. Notably, PBG proliferation index correlated significantly with total PBG mass ($r = 0.666$; $p = 0.003$).

PBG apoptosis was evaluated by IHC for cleaved caspase 3 and TUNEL assay (Figure 2B,C). PBG expression of cleaved caspase 3 was significantly higher in samples obtained from bile ducts from patients with NAS (score, 1.8 ± 0.6) or HAT (score, 1.9 ± 0.9), compared to controls (score, 0.6 ± 0.5; $p = 0.031$ and $p = 0.019$, respectively). In parallel, TUNEL assay confirmed a higher percentage of apoptotic PBG cells in NAS (47.9% ± 12.0%) or HAT (53.9% ± 4.8%), compared to controls (10.1% ± 6.8%; $p < 0.001$ and $p <$ 0.001, respectively), without significant differences
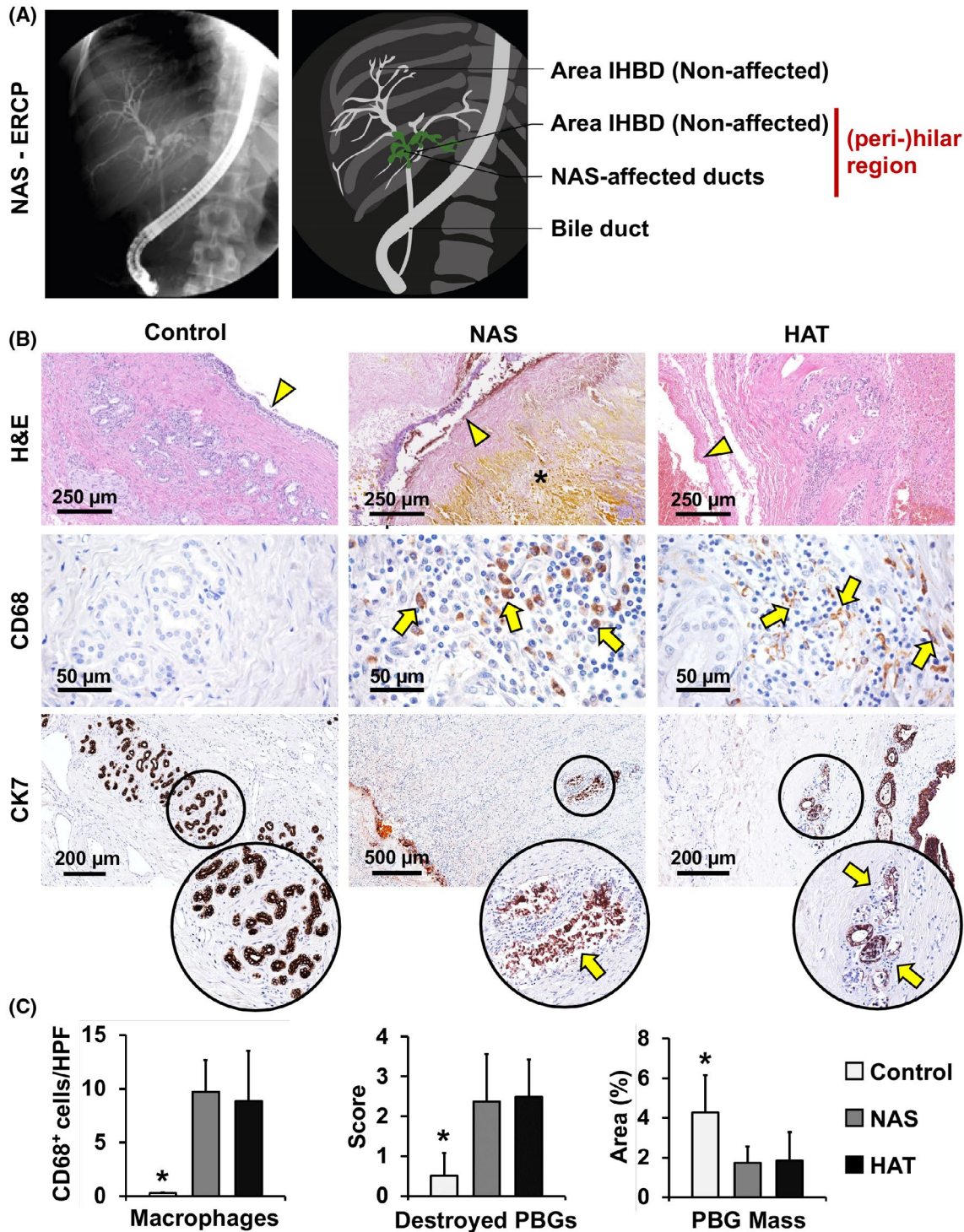
FIGURE 1 Radiological and microscopic presentation of NAS. (A) Endoscopic retrograde cholangiography (ERCP) showing NAS at the level of the hepatic duct and segmental intrahepatic bile ducts (green area), around the hilar region. (B) H&E stains (upper panels) and IHC for CD68 (middle panels) and CK7 (lower panels) of bile duct specimens obtained from patients retransplanted for nonbiliary causes (control), NAS, or HAT. In comparison to controls, bile ducts affected by NAS and HAT were characterized by loss of surface epithelium (arrowheads) and stroma destruction (asterisk). Infiltrating CD68$^+$ macrophages (arrows, middle panels) can be observed in NAS and HAT. In the lower panels, arrows indicate damaged PBGs in NAS and HAT, magnified in the circles below. (C) Histograms show quantification (mean and SD) of CD68$^+$ cells, destroyed PBGs, and PBG mass. *$p < 0.05$ versus other groups. Abbreviation: IHBD, intrahepatic bile duct

between the NAS and HAT groups. Finally, when cellular senescence was evaluated by IHC for γH2A.x, no significant differences were found between groups (Figure 2B,C). Additional immunostainings for senescence markers p16 and p21 confirmed that there were no notable differences between the groups (Figure S5).
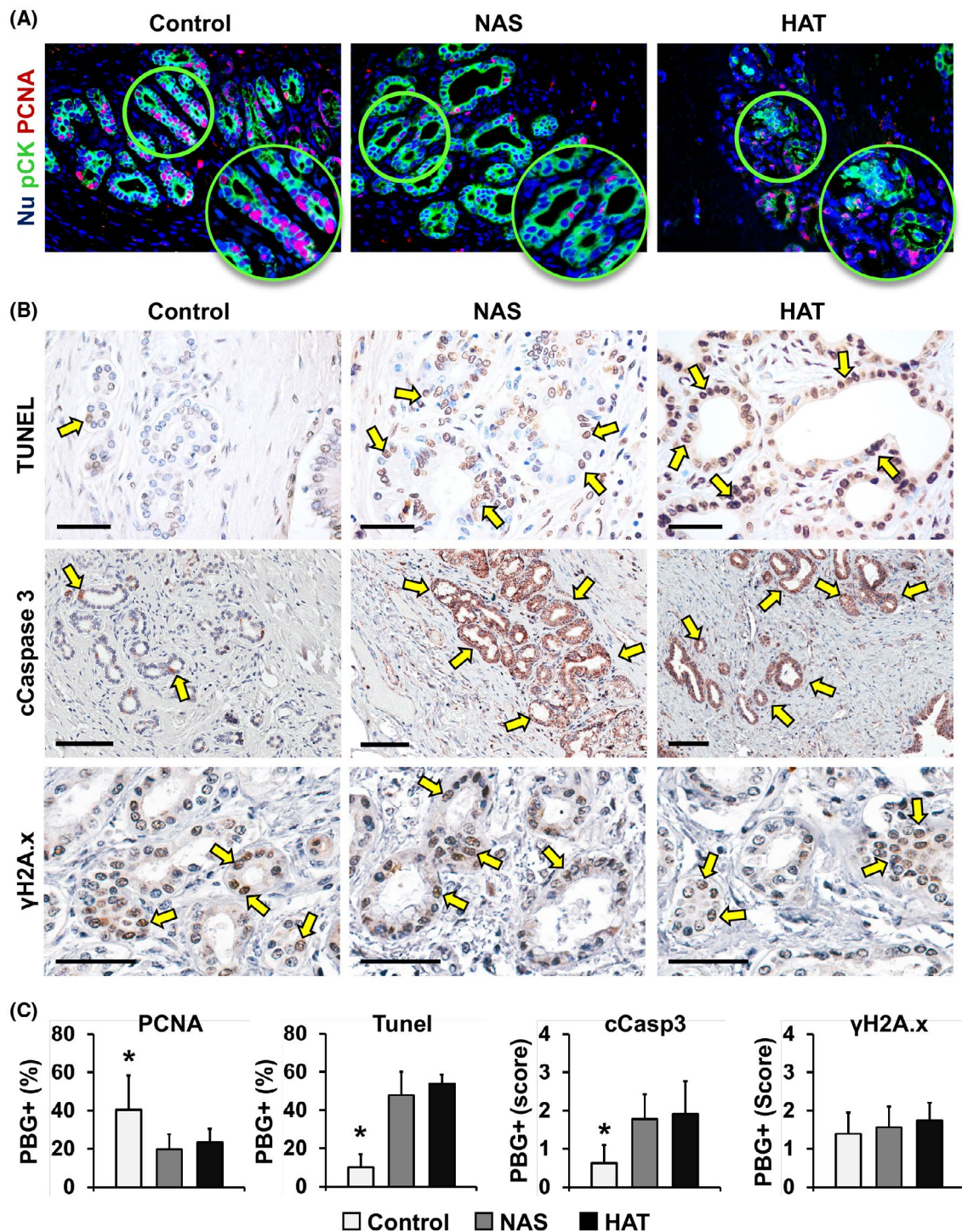
FIGURE 2 PBG proliferation, apoptosis, and senescence. (A) IF for pCK (green) and PCNA (red) of bile duct specimens obtained from patients retransplanted for nonbiliary causes (control), NAS, or HAT. Nuclei were counterstained with DAPI and are displayed in blue. (B) TUNEL assay (upper panels) and IHC for cleaved (c)Caspase 3 (middle panels) and γH2A.x (lower panels). Arrows indicate positive cells. Scale bars, 100 μm. (C) Histograms show quantification (mean and SD) for PCNA- (PBG proliferation index) and TUNEL-positive (PBG apoptosis) cells within PBGs and for the SQ score of cCaspase 3 (PBG apoptosis) and γH2A.x (PBG senescence). *$p < 0.05$ versus other groups

PBG phenotype in NAS and HAT

SRY-box transcription factor 9 (Sox9) was used as a stem/progenitor cell marker within PBGs (Figure 3A,F); Sox9 positivity was significantly lower in the NAS (11.7% ± 11.8%) and HAT (16.7% ± 17.1%) groups, compared to controls (42.6% ± 12.6%; $p = 0.010$ and $p = 0.034$, respectively). A significant correlation was found between the percentage of Sox9$^+$ cells and percentage of PCNA$^+$ cells within PBGs ($r = 0.772$; $p < 0.001$).
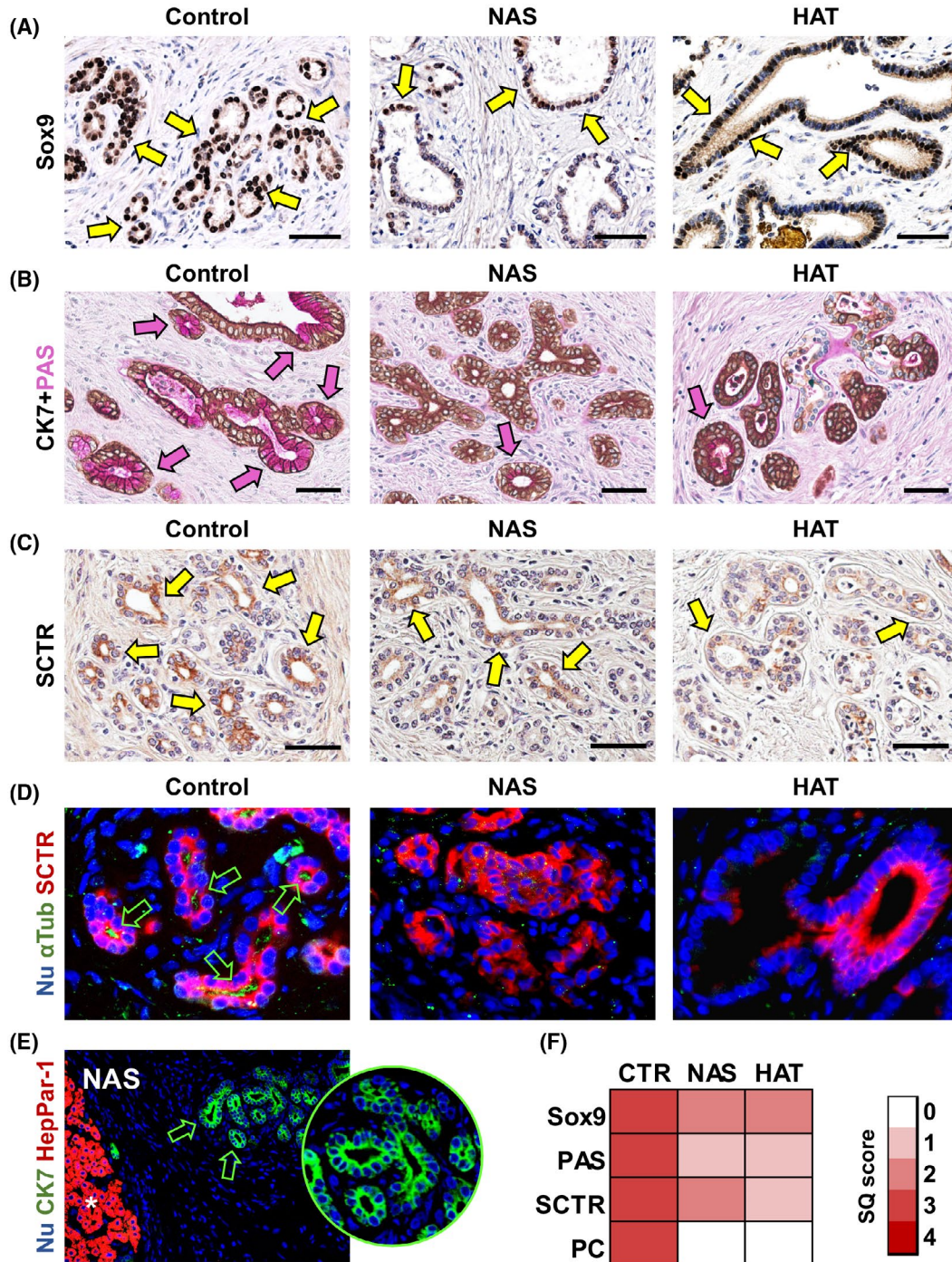
FIGURE 3 PBG cell phenotype. (A) IHC for transcription factor Sox9 in bile duct specimens obtained from patients retransplanted for nonbiliary causes (control), NAS, or HAT. Scale bars, 100 μm. (B) IHC for CK7 counterstained with PAS in control, NAS, and HAT groups. Scale bars, 50 μm. (C) IHC for SCTR in control, NAS, and HAT groups. Scale bars, 50 μm. (D) Double IF for α-acetylated tubulin (αTub; green) and SCTR (red) in control, NAS, and HAT groups. Green arrows indicate cells with primary cilium (PC). Original magnification: ×40. (E) IF for CK7 and HepPar1 in specimens of NAS-affected bile ducts. Original magnification: ×10. Asterisk indicates hepatocytes within liver parenchyma (positive control for HepPar1); PBGs are indicated by green arrows and magnified in the circle. (F) Heatmap reports SQ scores for Sox9, PAS, and SCTR positivity and cells with PC in PBGs. In (A-C), arrows indicate positive cells within PBGs. In (D-E), nuclei are counterstained with DAPI and displayed in blue. Abbreviations: CTR, control; Nu, nuclei

The number of PAS$^+$ mucous PBG cells (Figure 3B,F) was lower in NAS-affected (score, 1.4 ± 1.0) and the HAT-affected ducts (score, 1.3 ± 1.0), compared to controls (score, 3.0 ± 1.4; $p = 0.045$ and $p = 0.031$, respectively). To evaluate the commissioning of PBG cells toward a mature cholangiocyte fate, SCTR expression and the presence of primary cilia were investigated (Figure 3C,D,F). SCTR expression was lower

in the NAS (score, 1.5 ± 0.5) and HAT (score, 0.8 ± 0.6) groups, compared to the control group (score, 2.7 ± 1.2; p = 0.047 and p = 0.002, respectively) which was corroborated by relative SCTR RNA expression (Figure S4C). To examine the presence of primary cilia in PBG cells, we performed IF staining for α-acetylated tubulin as a marker of primary cilia (Figure 3D,F). The number of cells displaying a primary cilium was extremely reduced in ducts with NAS (score, 0.9 ± 0.8) or HAT (score, 0.6 ± 0.8), compared to controls (score, 2.5 ± 1.3; p = 0.014 and p = 0.009, respectively), whereas there was no difference between the NAS and HAT groups. Interestingly, in histological specimens from patients with NAS, nonaffected ducts were characterized by a similar percentage of PAS$^+$ (score, 2.5 ± 1.5) and SCTR$^+$ (score, 2.5 ± 0.5) cells within their PBGs as in controls (not shown).

Given that PBG cells in the NAS and HAT groups express less mature cholangiocyte traits, we explored the possibility that PBGs would be committed to a hepatocyte fate (Figure 3E); however, the hepatocyte marker, hepatocyte paraffin 1 (Hep-Par1), was negative in PBG cells in all examined samples.

Increased collagen deposition and myofibroblast activation in NAS

To evaluate fibrosis in the bile duct wall, we analyzed SR/FG-stained and Masson's trichrome–stained sections (Figure 4A,B and Figure S6). Average bile duct wall thickness appeared greater in patients with NAS (505 ± 130 μm), compared to the HAT group (184 ± 63 μm; p = 0.002) or controls (172 ± 68 μm; p = 0.002). No differences were found between HAT and controls. More specifically, when collagen fibers were evaluated, the extent of SR$^+$ fibers within the bile duct wall was higher in NAS (82.6% ± 2.9%) compared to HAT (75.0% ± 2.8%; p = 0.03) or control specimens (76.8% ± 2.4%; p = 0.03). No differences were found between HAT and controls. Duct wall fibrosis was inversely correlated with PBG mass (r = −0.519; p < 0.05).

Next, αSMA staining was used to evaluate myofibroblast activation in the bile duct wall and around PBGs (Figure 4A,B and Figure S7). The area occupied by αSMA-positive cells around PBGs was significantly higher in the NAS group (0.16 ± 0.05 μm^2/mm^2), but not in the HAT group (0.09 ± 0.11 μm^2/mm^2), compared to controls (0.04 ± 0.01 μm^2/mm^2; p < 0.05). Interestingly, in the NAS group, a concentric organization of myofibroblasts was observed around the PBGs. Moreover, in NAS patients, nonaffected ducts were characterized by a lower extent of αSMA$^+$ cells around PBGs (0.07 ± 0.012 μm^2/mm^2), compared to NAS-affected ducts (0.16 ± 0.06 μm^2/mm^2; p < 0.05).

To further characterize the activated myofibroblast population responsible for bile duct fibrosis in NAS, we performed stains in serial sections and IF for Thy-1 (thymus cell surface antigen 1; a specific marker for myofibroblasts) and neural cell adhesion molecule (NCAM; a specific marker for HSCs). Our analysis demonstrated that fibrogenetic cells in ducts affected by NAS were Thy-1$^+$/NCAM$^-$, indicating that the main contributors to the fibrotic process in NAS-affected ducts are (myo-)fibroblasts within the bile duct wall (Figure 4C and Figure S8). Finally, we investigated potential expression of profibrogenetic factors by PBGs that could activate myofibroblasts (Figure 4D and Figure S9), such as TGFβ1 and sonic hedgehog (SHH). In NAS and HAT, PBGs expressed higher levels of these factors (NAS, 2.4 ± 0.5 and 2.20 ± 0.40; HAT, 1.4 ± 0.6; 1.80 ± 0.50), compared to controls (0.4 ± 0.6; 0.20 ± 0.50; p < 0.05).

PVP injury and up-regulation of proangiogenic/hypoxia markers in NAS and HAT

Extension of the PVP and its modifications were studied by using the endothelial cell marker, vWF (Figure 5A,D). The number of microvessels (per microscopic field at 20×) within the entire bile duct wall was significantly lower in the NAS (17.3 ± 3.0) and HAT (11.2 ± 2.6) groups, compared to controls (25.4 ± 1.4; p < 0.001 and p < 0.001, respectively). Moreover, the MVD around PBGs was significantly reduced in the NAS (0.0044 ± 0.0017 μm^2/mm^2) and HAT (0.005 ± 0.001 μm^2/mm^2) groups, compared to controls (0.015 ± 0.008 μm^2/mm^2; p = 0.038 and p = 0.008, respectively). Moreover, quantitative PCR revealed that vWF expression on an RNA level was significantly lower in the NAS and HAT groups, with HAT showing the lowest expression (Figure S10A). These findings were confirmed by IHC for CD31 (Figure S11). To further characterize microvascular damage (Figure 5B,C,D), endothelial cell (EC) injury and apoptosis were evaluated. NAS and HAT showed higher degrees of EC injury (score in NAS, 1.6 ± 0.6; score in HAT, 2.6 ± 0.5) and a higher number of TUNEL$^+$ apoptotic ECs (score in NAS, 2.6 ± 0.6; score in HAT, 2.0 ± 1.0) compared to controls (score, 0.2 ± 0.4 and 0.6 ± 0.5; p < 0.05). Moreover, HAT presented with higher EC injury compared to NAS (p = 0.030), but no differences in EC apoptosis were found between these two groups.

We next examined the expression of key pathway elements in angiogenesis (i.e., VEGFs) and hypoxia (i.e., hypoxia inducible factor 1α [HIF-1α] and prolyl hydroxylase domain-containing protein 2 [PHD2]) in PBGs (Figure 6A-C). VEGF-A expression in PBGs was significantly higher in NAS-affected ducts (score, 2.3 ± 1.0), but not in HAT ducts (score, 0.9 ± 0.6), compared to controls (score, 0.7 ± 0.8; p = 0.03). This finding was supported by quantitative PCR, although not significant (Figure S10B).
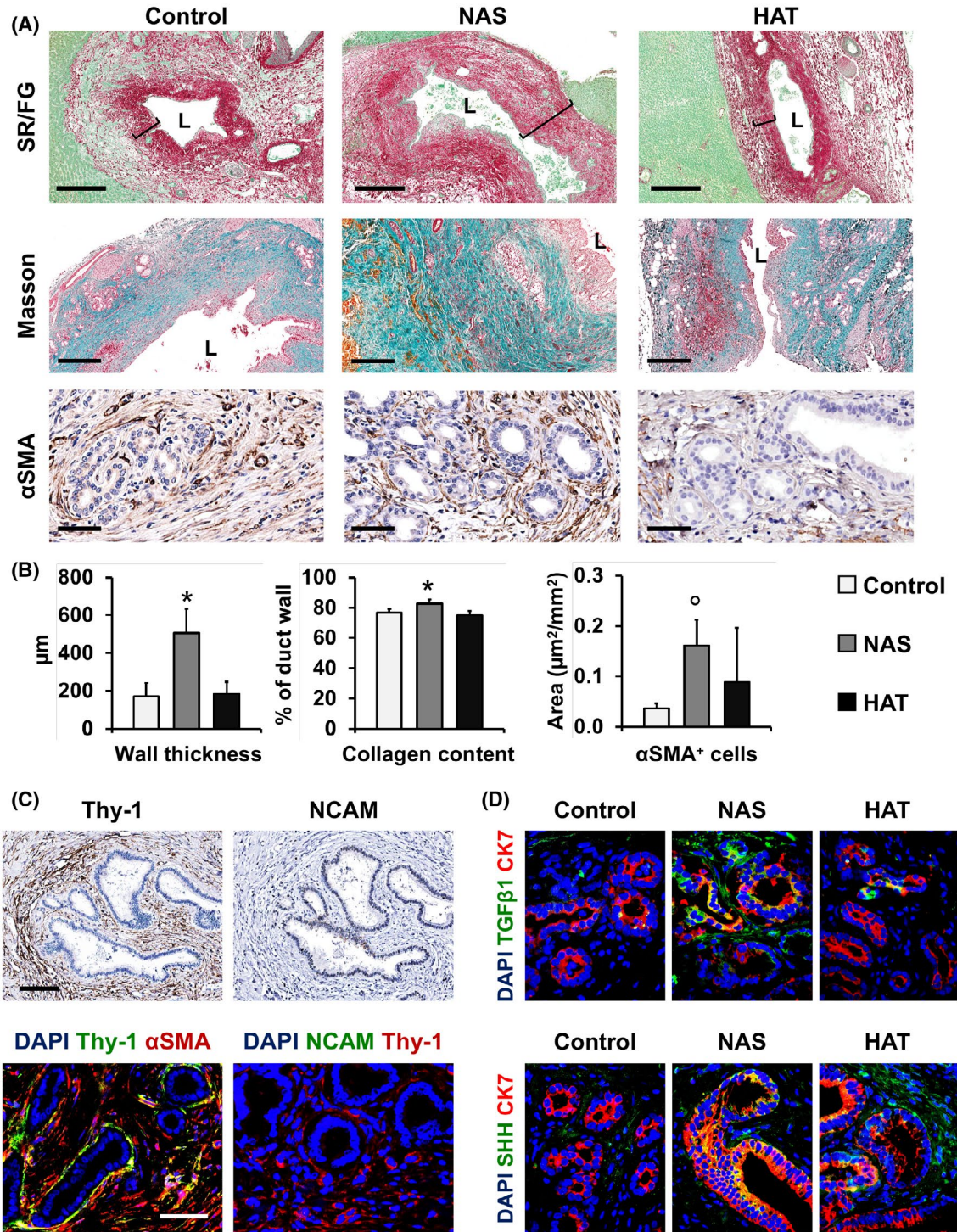
FIGURE 4 Collagen fiber deposition and myofibroblast activation. (A) SR/fast green (FG) stain (upper panels), Masson's trichrome stain (middle panels), and IHC for αSMA in bile duct specimens obtained from patients retransplanted for nonbiliary causes (control), NAS, or HAT. In (A), inset bars show the duct wall thickness. Scale bars, 500 μm (SR/FG and Masson) and 50 μm (αSMA). (B) Histograms show quantification (mean and SD) of duct wall thickness, collagen content of bile duct walls (expressed as percentage of bile duct wall), and of the number of αSMA$^+$ cells per mm^2 area around PBGs. *$p < 0.05$ versus other groups. (C) IHC on serial sections for Thy-1 and NCAM (upper panels) and double IF (lower panels) for Thy-1 and αSMA (left) and NCAM and Thy-1 (right) in NAS specimens. Scale bars, 100 μm (upper panels) and 50 μm (lower panels). (D) Double IF for TGFβ1 (green, upper panels) and SHH (green, lower panels) with CK7 (red) of control, NAS, and HAT groups. Original magnification: ×40. In (C,D), nuclei were counterstained with DAPI and are displayed in blue. Abbreviation: L, lumen
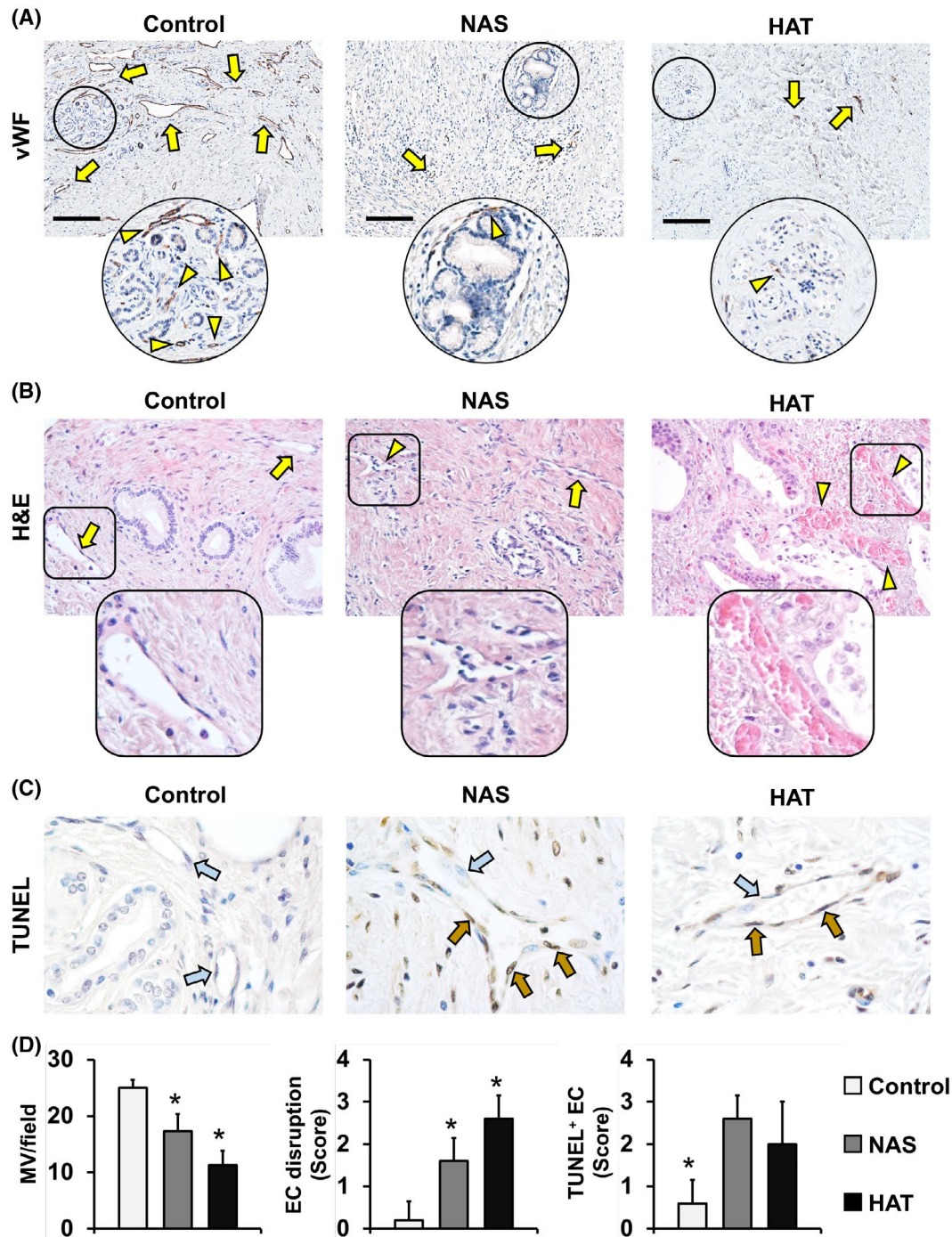
FIGURE 5 Modifications of the peribiliary vascular plexus. (A) IHC for vWF in bile duct specimens obtained from patients retransplanted for nonbiliary causes (control), NAS, or HAT. vWF+ vessels (arrows) and the MVD around PBGs (arrowheads) are shown. Areas in circles are magnified below. Scale bars, 200 μm. (B) H&E stains show normal vessels (arrows) and damaged ones (arrowheads) in the bile duct wall. Areas in squares are magnified below. Original magnification: ×20. (C) TUNEL assay shows nonapoptotic (blue arrows) and apoptotic (brown arrows) endothelial cells (ECs). Original magnification: ×40. (D) Histograms show quantification (mean and SD) of vWF+ microvessel (MV) density within bile ducts, score of EC disruption, and TUNEL+ ECs. *$p < 0.05$ versus other groups

VEGF-C expression was mostly negative in PBGs in all examined groups (Figure 6A). We next evaluated the expression of VEGF receptor 2 (VEGF-R2), the main VEGF-A receptor (Figure 6B). Within the bile duct walls, this marker was mainly expressed in blood vessels; the number of VEGF-R2-positive vessels was significantly reduced in HAT (2.2 ± 0.5) and NAS (4.3 ± 0.8) compared to controls (8.5 ± 0.4; $p < 0.05$). Accordingly, relative VEGF-R2 RNA expression was reduced in NAS and HAT samples compared to controls (Figure S10C).

HIF-1α expression (Figure 6C) was significantly higher in bile ducts of patients with NAS (score, 2.0 ± 1.0) or HAT (score, 1.6 ± 0.8), compared to controls (score, 0.7 ± 0.8; $p = 0.021$ and $p = 0.045$, respectively), which was confirmed on an RNA level (Figure S10D). Finally, the expression of PHD2 by PBG cells was significantly lower in NAS (score, 0.8 ± 1.0) and HAT (score, 1.0 ± 0.7) ducts compared to controls (score, 2.8 ± 0.8; $p = 0.012$ and $p = 0.024$, respectively) without significant differences between NAS and HAT groups.

Metabolome in human BTSCs differentiating into mature cholangiocytes

To evaluate whether stem cells modify their metabolism while differentiating into mature cholangiocytes, human BTSCs ($n = 5$ biological replicates) were cultured in self-replicating conditions (i.e., KM) and then transferred into a medium tailored for CholM for 14 days (Figure 6D). Culture media were collected after 14 days in KM (T1) and after 14 days in CholM (T2). Collected media were analyzed by NMR and explored by principal component analysis, producing a solution with two significant components, cumulatively explaining 85% of the total variance in the data (Figure 6D). From the analysis of loadings, a significant shift from a high- to a low-glycolytic phenotype was observed in human BTSCs in CholM compared to KM, as indicated by the negative correlation between glucose consumption (factor loading = −0.73) and lactate production (factor loading = +0.83) loadings: Glucose flux dropped off in CholM, leading to reduced lactate accumulation. The positive correlation pattern between glutamine consumption (factor loading = +0.80) and alanine (factor loading = +0.87) and lactate production loadings demonstrates a decrease in glutaminolysis flux, thus indicating a potential decreased flux through the alanine aminotransferase pathway to supply α-ketoglutarate to the tricarboxylic acid cycle. Figure 6D reports on metabolites with significant differences between T1 (KM) and T2 (CholM).

DISCUSSION

This study provides microscopic evidence that chronic local ischemia attributable to diminished bile duct microvasculature is a key mechanism underlying the pathogenesis of NAS after OLT. Because of the ongoing biliary hypoxia, the physiological regenerative process, originating from the BTSCs, residing in the PBGs, is compromised. Although grafts suffering from NAS, by definition, have a patent hepatic artery, the microscopic biliary and vascular abnormalities observed in these bile ducts were very similar to those observed after HAT. Despite the dual blood supply of the liver by the portal vein and hepatic artery, bile ducts are known to be largely dependent on the hepatic artery for the delivery of oxygen and nutrients. The main histological difference between bile ducts suffering from NAS or HAT was a significantly increased deposition of collagen matrix and activation of myofibroblasts in the former group, resulting in increased bile duct wall thickness and fibrosis. These signs of fibrotic wall thickening were in line with the radiological presentation of NAS, which was characterized by irregularities and narrowing of the donor bile ducts.

This study provides a detailed microscopic analysis of the bile ducts of donor livers suffering from NAS. In previous studies of biopsies taken from donor bile ducts at the time of OLT, it was noted that almost all transplanted organs have a substantial amount of bile duct injury after cold ischemic preservation.[6,20] This is characterized by loss of the surface epithelium, and a varying degree of injury of stroma cells, endothelium of the PVP, and epithelial cells of PBGs.[6] Although these alterations are frequently observed in bile ducts at the time of OLT, the majority of these organs do not develop NAS and show a complete regeneration of the bile duct wall, including PBG compartment, stroma, and vessels, as we observed in the control group included in this study. In contrast, cases that later developed NAS have been identified at the time of OLT by a more-severe injury of the PVP and extramural PBGs.[6] Given that PBGs are a niche of BTSCs from which the surface biliary epithelium can regenerate after severe injury, it has been suggested that insufficient regeneration is a key event underlying the pathogenesis of NAS.[6,9,20,21] However, formal evidence that bile ducts from liver grafts with end-stage NAS display features of a persistent hypoxic condition and insufficient regeneration has been lacking.

In the current study, we aimed to describe the microscopic phenotype of bile ducts that developed severe

FIGURE 6 Angiogenic response and metabolism of PBG cells. (A) IHC for VEGF-A (upper panels) and VEGF-C (lower panels) in bile duct specimens obtained from patients retransplanted for nonbiliary causes (control), NAS, or HAT. Heatmap reports SQ scores for VEGF-A and VEGF-C positivity in PBGs. Scale bars, 100 μm. (B) IHC for VEGF-R2. Original magnification: ×40. Histogram shows quantification (mean and SD) of VEGF-R2$^+$ vessels per high-power field (40×). *$p < 0.05$ versus other groups. (C) IHC for HIF-1α (upper panels) and PHD2 (lower panels). Scale bars, 100 μm. Heatmap shows SQ scores for HIF-1α and PHD2 expression in PBGs. (D) Human biliary tree stem/progenitor cells (hBTSCs) were cultured in self-replicating conditions (KM) for 14 days (T1) and then transferred in a medium tailored for CholM for another 14 days (T2). Metabolites in collected media were analyzed by NMR and explored by principal component (PC) analysis, producing a solution with two significant components, cumulatively explaining 85% of the total variance in the data. The histogram shows quantification (means and SD) of metabolites in culture medium with significant differences comparing T1 with T2. Abbreviation: CTR, control
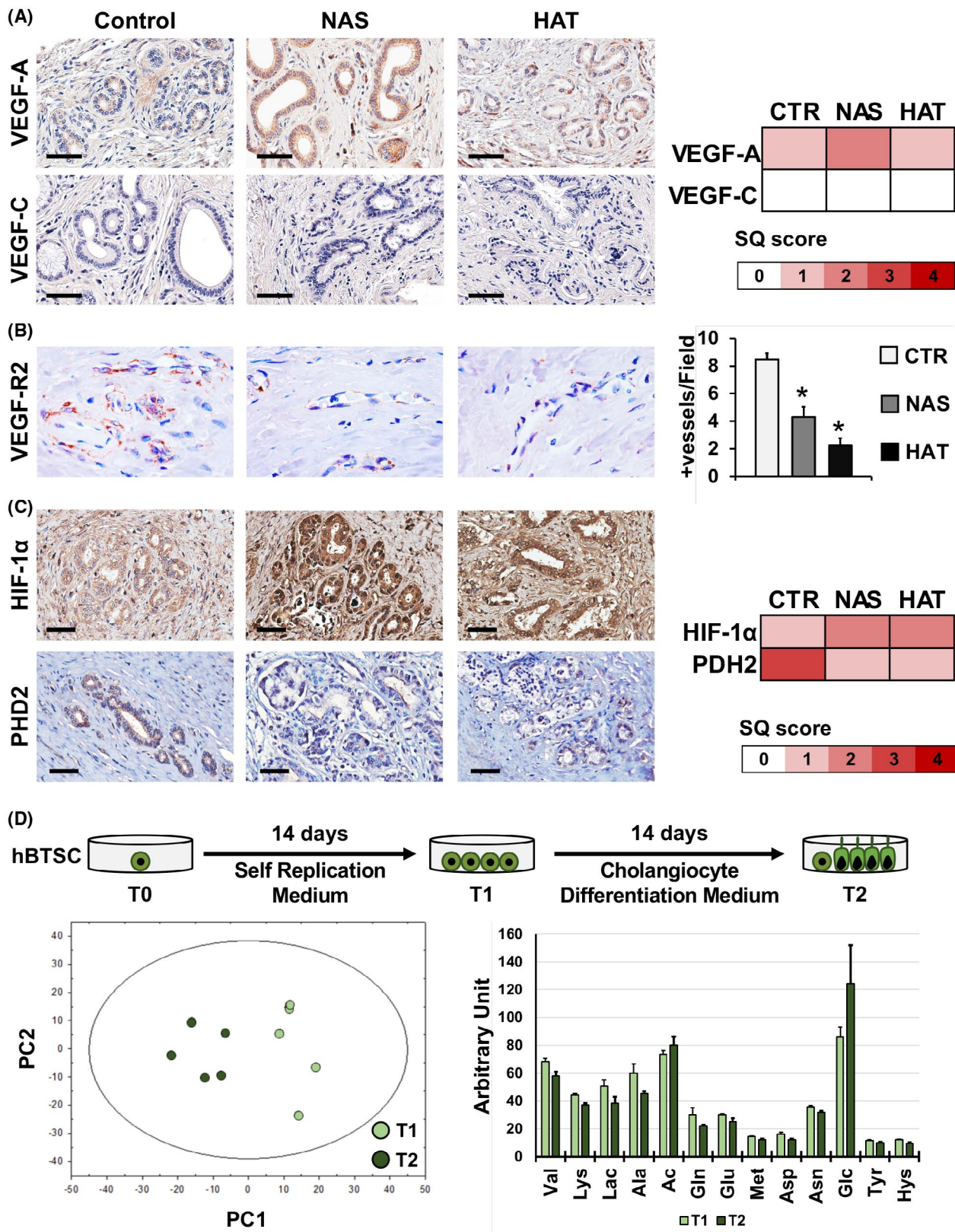
NAS, requiring retransplantation of the liver. We hypothesized that these bile ducts would have evidence of ongoing hypoxia and lack of regeneration from PBG stem/progenitor cells. As positive and negative controls of hypoxia, we used bile ducts from livers that required retransplantation for early HAT or nonbiliary causes of graft failure, such as recurrent viral or autoimmune hepatitis. By using these control groups, we were able to demonstrate that the bile duct injury observed in NAS is indeed compatible with (ongoing) hypoxia after the OLT

procedure, despite a patent hepatic artery. Bile ducts of livers that required retransplantation for nonbiliary and -ischemic causes of graft failure had normal microscopic architecture, characterized by intact surface epithelium and healthy appearing PVP and PBGs. Biliary epithelial cells in these ducts appeared to be successfully regenerated and restored posttransplantation. In contrast to this, bile ducts with NAS or HAT had evidence of a diminished MVD, altered expression of hypoxia pathway elements (i.e., HIF-1α and its regulator, PHD2),[22] reduced PBG mass, and increased PBG apoptosis. In parallel with this, we found evidence of reduced PBG stem/progenitor cell proliferation and diminished differentiation toward mature cells (mucus production, secretin receptor expression, and presence of primary cilia) in bile ducts with NAS or HAT, compared to controls.

The only two differences between bile ducts affected by NAS and HAT were increased fibrosis and VEGF-A expression in ducts with NAS, but not in those with HAT. Bile ducts with NAS displayed markedly increased deposition of collagen and myofibroblast activation, resulting in wall thickening. Our data suggest that hypoxic damage of PBGs could trigger the expression of profibrogenetic factors, such as TGFβ1 and SHH, which can activate myofibroblasts in a paracrine fashion. Differences in bile duct wall fibrosis between NAS and HAT could be explained by the longer time interval between the first transplant and retransplantation in the NAS group, compared to the HAT group. We intentionally selected only bile ducts with early HAT (<40 days), given that HAT occurring at a longer time interval after OLT does not always lead to clinically overt bile duct ischemia because arterial collaterals may have been developed in this situation.[23] Therefore, in contrast to early HAT, late HAT frequently does not require retransplantation.[24]

The microscopic picture of bile duct wall fibrosis and thickening matched the one of radiological imaging, which was characterized by irregularities and narrowing of the donor bile ducts. NAS typically affects the extrahepatic common bile duct, hepatic ducts, and the segmental intrahepatic donor bile ducts, whereas smaller intrahepatic branches are usually spared.[4] In accordance with the radiological presentation of NAS, we identified relatively well preserved and healthy appearing area, septal, and interlobular bile duct branches in the same sections as the affected bile ducts. PBGs in the nonaffected branches were not histomorphologically different from those in control bile ducts. These findings confirm that posttransplant NAS mainly occurs in the extrahepatic common bile duct, hepatic ducts, and the segmental intrahepatic donor bile ducts. Of note, previous work demonstrated that DCD organs are more prone to develop NAS and show increased damage of PBGs during the transplant procedure.[25] In our cases, no significant differences were found among NAS patients when comparing bile duct samples of patients who received a DBD versus DCD organ. Therefore, the number of DCD organs in the NAS group did not influence our analysis. However, further studies on a larger population will be needed to thoroughly assess the presence of specific characteristics of NAS in DCD versus DBD donors.

The difference in VEGF-A expression in PBGs of bile ducts with NAS or HAT is remarkable. Both bile ducts affected by NAS or HAT displayed increased PBG expression of HIF-1α, but VEGF-A expression was only increased in NAS. A possible explanation for this is the presence of chronic (ongoing) biliary hypoxia in bile ducts that develop NAS, compared to the more acute hypoxia after HAT.[4,23] Increased VEGF-A expression in PBG cells of bile ducts with NAS could represent a compensatory response to overcome the prolonged biliary hypoxia.[26] Residual PBGs both in HAT- and NAS-affected ducts showed negligible signs of mature cholangiocyte commitment. In line with this, our in vitro study using isolated human BTSCs demonstrated that the metabolomic profile of BTSCs shifts from a glycolytic metabolism in self-replication conditions to an oxidative one as differentiation to mature cholangiocytes takes place. The basal glycolytic metabolism in human BTSCs within PBGs could explain their relative resistance to ischemia-reperfusion injury during the transplant procedure, compared to cholangiocytes lining the surface epithelium.[27,28] Interestingly, human BTSC differentiation into mature cholangiocytes was associated with the inhibition of glutaminolysis and the consumption of amino acids, likely for anabolic purposes. Thus, differentiation and anabolic reconstruction—which are essential elements of regeneration—may be impeded in PBGs in NAS-affected ducts because of ongoing oxygen shortage (i.e., hypoxia).[29] Several studies in experimental models demonstrated that bile duct regeneration is supported by preservation of the PVP and that hepatic artery ligation impairs biliary epithelial cell proliferation.[26] In line with this, our study further highlights the importance of the PVP in biliary regeneration. Insufficient and timely restoration of the bile duct microvasculature after OLT results in ongoing local hypoxia, leading to lack of biliary regeneration and subsequent fibrotic narrowing of the bile ducts. This implies that optimal preservation of the PVP should be a key target of liver graft preservation before OLT.

In an *ex vivo* model of human bile duct regeneration after cold ischemia-induced injury, using precision-cut bile duct slices, we previously demonstrated that BTSCs residing in the PBGs are able to respond to bile duct epithelial loss with proliferation, differentiation, and maturation to restore epithelial integrity.[9] In accordance with the current in vivo findings, bile duct regeneration in the *ex vivo* model was accompanied by increased expression of HIF-1α and VEGF-A. Moreover, in the *ex vivo* model, regeneration was accompanied by

myofibroblast activation and increased collagen deposition in the stroma in a concentric fashion around the PBGs. These changes in bile duct matrix were also observed in the current clinical study and likely contributed to stricture formation.

A limitation of this study could reside in the lack of data from PBG cells directly isolated from diseased organs. A full molecular study of isolated cells would furnish further insights in the pathogenesis of this disease. However, such analysis could represent an obstacle for successive studies given the difficulties in tissue procurement and the presence of a fibrosis niche around PBGs in NAS-affected ducts, which would make the isolation of viable cells difficult.

In conclusion, our findings suggest that persistent biliary hypoxia attributable to loss of microvasculature is a key mechanism underlying the development of NAS after OLT. NAS-affected ducts are characterized by a histomorphological phenotype of chronic biliary hypoxia attributable to loss of microvasculature/PVP, resulting in reduced proliferation and differentiation of PBG stem/progenitor cells into mature cholangiocytes. The absence of a regenerative response is accompanied by increased fibrosis of the bile duct wall, compatible with the radiological presentation of bile duct strictures. Optimal preservation of the PVP should therefore be a key target in donor organ preservation to avoid the development of NAS after OLT.

ETHICAL STATEMENT

Clinical data of donors and recipients were collected from the local transplant databases and individual electronic patient files. All tissue specimens were anonymously coded. Anonymized analysis of data and biomaterials was allowed as part of the TransplantLines cohort study (NCT03272841).[30] Patients that signed the objection form were excluded from this study. Protocols conformed to the ethical guidelines of the 1975 Declaration of Helsinki and were approved by the local institutional review boards (Sapienza University of Rome, Rome, Italy[17,31] and METc UMCG 2017/638, registration number: 202000462; UMCG, Groningen, The Netherlands). No donor organs were obtained from executed prisoners or other institutionalized persons.

CONFLICT OF INTEREST
Nothing to report.

AUTHORS CONTRIBUTIONS
Robert J. Porte had the initial conception for the study. Iris E. M. de Jong and Diletta Overi contributed by performing experiments and image analyses. Both were involved in the data interpretation. Guido Carpino contributed to the design of the study, oversaw all the experiments, and contributed to the image analyses and data interpretation. Vincenzo Cardinale and Luca Casadei contributed to the manuscript with the exo-metabolomics of isolated human BTSCs. Carmine Mancone contributed by performing experiments. Annette S. H. Gouw and Marius C. van den Heuvel performed the pathological evaluation of H&E stains. Léon C. van Kempen performed the qPCR experiments. The first drafts of the manuscript were written by Iris E. M. de Jong, Robert J. Porte, and Guido Carpino. Funding derived from grants obtained by Eugenio Gaudio, Domenico Alvaro, and Paolo Onori. All authors reviewed the manuscript and edited the text.

ORCID
Diletta Overi https://orcid.org/0000-0003-3561-8903
Guido Carpino https://orcid.org/0000-0001-8570-2519

REFERENCES
1. Kochhar G, Parungao JM, Hanouneh IA, Parsi MA. Biliary complications following liver transplantation. World J Gastroenterol. 2013;19:2841–6.
2. de Vries Y, von Meijenfeldt FA, Porte RJ. Post-transplant cholangiopathy: classification, pathogenesis, and preventive strategies. Biochim Biophys Acta Mol Basis Dis. 2018;1864:1507–15.
3. Guichelaar MMJ, Benson JT, Malinchoc M, Krom RAF, Wiesner RH, Charlton MR. Risk factors for and clinical course of non-anastomotic biliary strictures after liver transplantation. Am J Transplant. 2003;3:885–90.
4. Buis CI, Verdonk RC, der Jagt V, Eric J, van der Hilst CS, Slooff MJH, et al. Nonanastomotic biliary strictures after liver transplantation, part 1: radiological features and risk factors for early vs. late presentation. Liver Transpl. 2007;13:708–18.
5. Buis CI, Geuken E, Visser DS, Kuipers F, Haagsma EB, Verkade HJ, et al. Altered bile composition after liver transplantation is associated with the development of nonanastomotic biliary strictures. J Hepatol. 2009;50:69–79.
6. op den Dries S, Westerkamp AC, Karimian N, Gouw ASH, Bruinsma BG, Markmann JF, et al. Injury to peribiliary glands and vascular plexus before liver transplantation predicts formation of non-anastomotic biliary strictures. J Hepatol. 2014;60:1172–9.
7. Gaudio E, Onori P, Pannarale L, Marinozzi G. Microcirculation of the extrahepatic biliary tree: a scanning electron microscopy study of corrosion casts. J Anat. 1993;182(Pt. 1):37–44.
8. Castaing D. Surgical anatomy of the biliary tract. HPB (Oxford). 2008;10:72–6.
9. de Jong IEM, Matton APM, van Praagh JB, van Haaften WT, Wiersema-Buist J, van Wijk LA, et al. Peribiliary glands are key in regeneration of the human biliary epithelium after severe bile duct injury. Hepatology. 2019;69:1719–34.
10. Carpino G, Cardinale V, Onori P, Franchitto A, Berloco PB, Rossi M, et al. Biliary tree stem/progenitor cells in glands of extrahepatic and intrahepatic bile ducts: an anatomical in situ study yielding evidence of maturational lineages. J Anat. 2012;220:186–99.
11. DiPaola F, Shivakumar P, Pfister J, Walters S, Sabla G, Bezerra JA. Identification of intramural epithelial networks linked to peribiliary glands that express progenitor cell markers and proliferate after injury in mice. Hepatology. 2013;58:1486–96.

12. Carnevale G, Carpino G, Cardinale V, Pisciotta A, Riccio M, Bertoni L, et al. Activation of Fas/FasL pathway and the role of c-FLIP in primary culture of human cholangiocarcinoma cells. Sci Rep. 2017;7:14419.

13. Carpino G, Nevi L, Overi D, Cardinale V, Lu WY, Di Matteo S, et al. Peribiliary gland niche participates in biliary tree regeneration in mouse and in human primary sclerosing cholangitis. Hepatology. 2020;71:972–89.

14. Carpino G, Cardinale V, Renzi A, Hov JR, Berloco PB, Rossi M, et al. Activation of biliary tree stem cells within peribiliary glands in primary sclerosing cholangitis. J Hepatol. 2015;63:1220–8.

15. Carpino G, Cardinale V, Folseraas T, Overi D, Floreani A, Franchitto A, et al. Hepatic stem/progenitor cell activation differs between primary sclerosing and primary biliary cholangitis. Am J Pathol. 2018;188:627–39.

16. Pfaffl MW. A new mathematical model for relative quantitative in real-time RT-PCR. Nucleic Acids Res. 2001;29:e45.

17. Costantini D, Overi D, Casadei L, Cardinale V, Nevi L, Carpino G, et al. Simulated microgravity promotes the formation of tridimensional cultures and stimulates pluripotency and a glycolytic metabolism in human hepatic and biliary tree stem/progenitor cells. Sci Rep. 2019;9:5559.

18. Carpino G, Cardinale V, Gentile R, Onori P, Semeraro R, Franchitto A, et al. Evidence for multipotent endodermal stem/progenitor cell populations in human gallbladder. J Hepatol. 2014;60:1194–202.

19. Casadei L, Valerio M. (1)H NMR metabolomic footprinting analysis for the in vitro screening of potential chemopreventive agents. Methods Mol Biol. 2016;1379:89–97.

20. Karimian N, Op den Dries S, Porte RJ. The origin of biliary strictures after liver transplantation: is it the amount of epithelial injury or insufficient regeneration that counts? J Hepatol. 2013;58:1065–7.

21. Sutton ME, Dries S, Koster MH, Lisman T, Gouw ASH, Porte RJ. Regeneration of human extrahepatic biliary epithelium: the peribiliary glands as progenitor cell compartment. Liver Int. 2012;32:554–9.

22. Epstein ACR, Gleadle JM, McNeill LA, Hewitson KS, O'Rourke J, Mole DR, et al. *C. elegans* EGL-9 and mammalian homologs define a family of dioxygenases that regulate HIF by prolyl hydroxylation. Cell. 2001;107:43–54.

23. Frongillo F, Lirosi MC, Nure E, Inchingolo R, Bianco G, Silvestrini N, et al. Diagnosis and management of hepatic artery complications after liver transplantation. Transplant Proc. 2015;47:2150–5.

24. Pareja E, Cortes M, Navarro R, Sanjuan F, López R, Mir J. Vascular complications after orthotopic liver transplantation: hepatic artery thrombosis. Transplant Proc. 2010;42:2970–2.

25. Franchitto A, Overi D, Mancinelli R, Mitterhofer AP, Muiesan P, Tinti F, et al. Peribiliary gland damage due to liver transplantation involves peribiliary vascular plexus and vascular endothelial growth factor. Eur J Histochem. 2019;63:3022.

26. Gaudio E, Barbaro B, Alvaro D, Glaser S, Francis H, Franchitto A, et al. Administration of r-VEGF-A prevents hepatic artery ligation-induced bile duct damage in bile duct ligated rats. Am J Physiol Gastrointest Liver Physiol. 2006;291:G307–17.

27. Fujiwara H, Tateishi K, Misumi K, Hayashi A, Igarashi K, Kato H, et al. Mutant IDH1 confers resistance to energy stress in normal biliary cells through PFKP-induced aerobic glycolysis and AMPK activation. Sci Rep. 2019;9:18859.

28. Ryall JG, Cliff T, Dalton S, Sartorelli V. Metabolic reprogramming of stem cell epigenetics. Cell Stem Cell. 2015;17:651–62.

29. Gaudio E, Franchitto A, Pannarale L, Carpino G, Alpini G, Francis H, et al. Cholangiocytes and blood supply. World J Gastroenterol. 2006;12:3546–52.

30. Eisenga MF, Gomes-Neto AW, van Londen M, Ziengs AL, Douwes RM, Stam SP, et al. Rationale and design of TransplantLines: a prospective cohort study and biobank of solid organ transplant recipients. BMJ Open. 2018;8:e024502.

31. Wang Y, Lanzoni G, Carpino G, Cui CB, Dominguez-Bendala J, Wauthier E, et al. Biliary tree stem cells, precursors to pancreatic committed progenitors: evidence for possible life-long pancreatic organogenesis. Stem Cells. 2013;31:1966–79.

SUPPORTING INFORMATION

Additional supporting information may be found in the online version of the article at the publisher's website.